Functional Localization Based on Measurements with a Whole-Head Magnetometer System

Matti S. Hämäläinen*

Summary: Whole-cortex magnetometers represent a significant methodological breakthrough in noninvasive studies of the brain's electrical activity. This paper describes our 122-channel instrument with planar gradiometers, methods to interpret its data, and gives a few examples of neuromagnetic studies.

Key words: Neuromagnetism; SQUID; Inverse problem; Functional imaging.

Introduction

It was proposed already in the early days of neuromagnetic studies that the ultimate instrument for the detection of the brain's magnetic fields will cover the whole cortex simultaneously, with a sufficient number of sensors to capture all the details of the field distribution. Here we describe such an instrument, which has been operational for about two years, including aspects of data interpretation, and give a few representative examples.

The 122-channel gradiometer

Our 122-SQUID system has been operational since June 1992 (Ahonen et al. 1993a). This Neuromag-122 system (Neuromag Ltd., Helsinki, Finland) consists of 122 planar gradiometers arranged in 61 pairs, measuring the two orthogonal tangential derivatives, $\partial B_z / \partial x$ and $\partial B_z / \partial y$, of the field component B_z, normal to a helmet-shaped surface approximating the shape of the head (figure 1).

The thin-film superconducting pickup coils are deposited on 28 x 28 mm^2 silicon chips. The separation of the double-sensor units is approximately 40 mm. As discussed in Ahonen et al. (1993b), this setup corresponds to a conventional axial gradiometer sampling grid which is denser by a factor of $\sqrt{2}$. The electronics is based on direct readout with amplifier noise cancellation (Seppä et al. 1991). This eliminates the need for separate preamplifiers; the entire electronics is located outside the magnetically shielded room.

Our sensor arrangement has several advantages over the traditional axial gradiometer array: 1) The coils can be manufactured easily using precise thin-film techniques with very good inherent gradiometer balance. The entire two-channel gradiometer component can be produced in large quantities and tested thoroughly before assembly. 2) The radial space required by the planar array is small, resulting in a compact construction of the dewar. 3) The planar gradiometer has maximum sensitivity to sources directly below it. This has turned out to be very important where several sources are simultaneously active. It is also evident that a very clear picture emerges when spontaneous activity is being studied.

Source identification

Owing to the limited coverage of magnetometers used in the past, many neuromagnetic studies have concentrated on pinpointing the locations of only a few active cortical sites at a time. A vast majority of the studies have dealt with primary projection areas whose approximate location has been known *a priori*.

With whole-head covering systems, more complicated experiments can be conducted readily. For example, we have studied the sequence of brain activity following a visual presentation of objects when the subject was asked to name them either silently or aloud (see Salmelin et al. 1994). Optimally, one would be able to find the locations

*Low Temperature Laboratory, Helsinki University of Technology, Finland.

Accepted for publication: January 30, 1995.

This paper describes work which is undertaken in our laboratory in a multidisciplinary team lead by Professors Olli V. Lounasmaa and Riitta Hari. I am grateful to Riitta Salmelin and Olli V. Lounasmaa for comments on this manuscript.

Correspondence and reprint requests should be addressed to Matti S. Hamalainen, Low Temperature Laboratory, Helsinki University of Technology, 02150 Espoo, Finland.

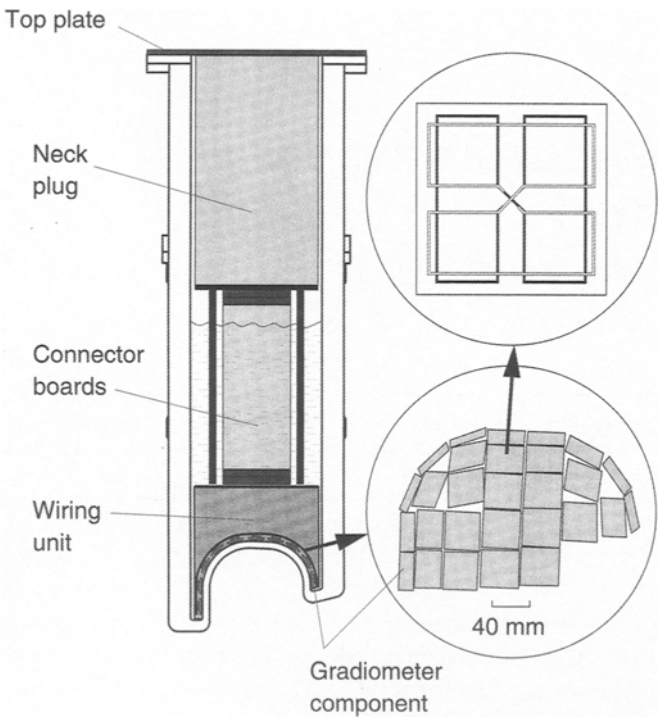

Figure 1. Left: The 122-channel gradiometer probe unit comprising the dewar and the three-module insert structure. The subject leans against the helmet-shaped bottom part of the dewar. Right above: Schematic illustration of the dual gradiometer chip with orthogonal figure-of-eight shaped pick-up coils. Right below: The helmet-like layout of the sensor units.

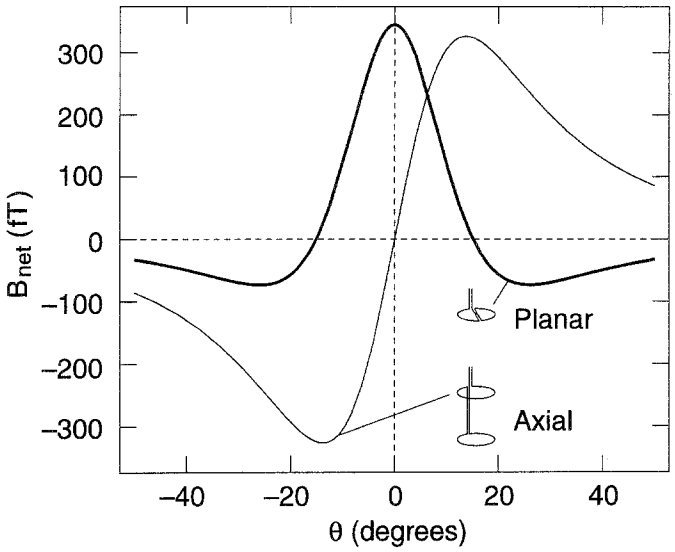

Figure 2. Amplitudes of magnetic signals due to a tangential current dipole in a spherically symmetric volume conductor. B_{net}, the difference signal between the gradiometer loops, is calculated on a circle over the dipole, perpendicular to its direction. An axial first-order gradiometer and a planar first-order gradiometer are considered. The radius of the spherical surface along which the measurements are performed is 100 mm and the dipole is assumed to be located 30 mm below the surface. The dipole moment is 10nAm and the base lengths of the axial and planar gradiometers are 60 mm and 15 mm, respectively. Note that for the planar gradiometer the maximum signal is obtained just above the source.

of the sources and their time courses in such a complex experiment automatically, without any manual intervention. However, owing to the nonuniqueness of the electromagnetic inverse problem this goal is very difficult to achieve. The present section describes some methods we routinely employ to indentify the sources of measured signals.

Selective sensitivity of the planar gradiometer

The planar gradiometer produces the maximum signal just above a dipolar current source, in contrast to the two maxima appearing in the pattern recorded by an axial gradiometer, see figure 2. Therefore, we can often directly infer the activated sites already in the spontaneous raw data or in the averaged evoked responses. The approximate result of the study can be inferred already during data acquisition and is very helpful especially in studies of patients.

With several asynchronous sources it is likely that their field patters overlap significantly when recorded with an axial gradiometer array. Therefore, the pattern provided by measures like power spectra may be very misleading, showing, for example, two maxima, separated by a large distance when two sources are asynchronously active. In contrast, the power spectrum pattern calculated from planar gradiometer recordings is much easier to understand with a maximum above each active area only.

In addition, each planar gradiometer pair records two independent signals corresponding to the two orthogonal source orientations under the sensor. If the two temporal waveforms recorded by a gradiometer pair are not directly proportional, we can readily conclude that at least two sources with uncorrelated time courses are required to explain the measured data.

Selective source localization

If the data can be explained by a single dipole it is usually easy to provide an initial guess for the least-squares fit automatically. With our planar gradiometer we place the initial source under the sensor showing maximum signal at a depth of a few centimeters under

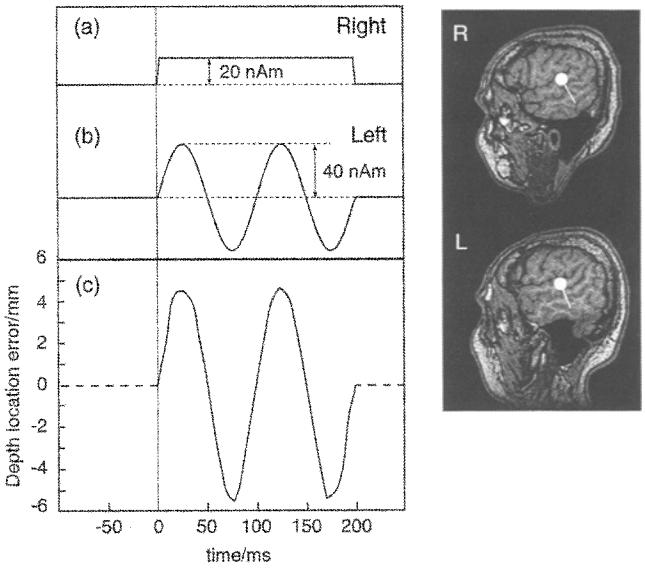

Figure 3. Illustration of source interactions. Left: (a) and (b) The assumed waveforms of the sources in the right and left auditory cortices. (c) The depth location error for the right-hemisphere source when it was modelled without using the signals measured over the left hemisphere. Right: The locations of the model sources displayed on sagittal MR images.

the scalp. In a multidipole fit the situation is more complicated. If the initial source locations are not appropriately chosen, the fit may not converge to the global minimum. Therefore, we use a manually guided fitting for multiple sources. We select several subsets of channels and perform first a single-dipole fit to each selection. The dipoles found are used as initial guesses in a complete multi-dipole fit routine. For example, when auditory evoked fields are analyzed, we select 30-40 channels from each hemisphere in turn and, thereby, find the approximate locations of, say, the N100m sources in each hemisphere. Thereafter, we include all channels to fit both N100m sources simultaneously.

Interactions of distant sources

The distribution of the normal magnetic field component is orthogonal to the corresponding pattern of the electric potential produced by a current dipole and, as a first approximation, unaffected by the layered conductivity structure of the head. Furthermore, the magnetic pattern is more compact than the electric one, whereby the fields of two simultaneously active sources are less likely to overlap. These features make it particularly easy to study the signals from the two auditory cortices and have also enabled a clear identification of the second somatosensory cortex, SII.

However, with our whole-cortex magnetometer we have noted that the distributions resulting from the simultaneous activation of the left and right auditory cortices overlap enough to affect the precise localization of the sources. As a result, a two-dipole fit to the complete data is different from two single dipole fits to a selection of channels over each hemisphere. The difference of source locations of the calculated N100m deflection typically amounts to 3-5 mm. The change is approximately normal to the surface of the head.

This may become important if small differences in source locations under different conditions are considered. If the field is recorded over one hemisphere only, one may find a misleading change in source depth which is actually due to a change in the strength of the source in the opposite hemisphere.

To quantify this overlap effect we conducted the following simulation: 1) The N100m was modelled with two dipoles, one in each hemisphere. 2) The source locations from this fit to actual data were employed to produce simulated signals. The amplitude of the right-hemisphere source was kept constant, Q=20nAm, over t=0...200 ms while the amplitude of the left-hemisphere source was sinusoidally varying, f=10 Hz, with an amplitude of Q=40nAm. 3) The simulated data over the right hemisphere were used to fit a single moving dipole at 1 ms intervals.

As shown in figure 3, the amplitude variation of the left-hemisphere source is reflected on the right hemisphere with an apparent depth movement of about ±5mm. Since the location of the left-hemisphere source cannot be reliably determined on the basis of right-hemisphere data only, this systematic error cannot be corrected by adding a second dipole without measurements over the left hemisphere.

The projection method

Analyses of brain electromagnetic signals using linear decompositions has become very popular, especially in the context of time-varying dipole modelling (Scherg 1990; Mosher 1992). We have recently widened the scope of this approach to include in component signals which can not be described easily as a combination of signal vectors arising from current dipoles (Uusitalo et al. 1994).

Signal space and projection operators

A set of m linearly independent n-channel magnetic field signals $\mathbf{b}_1,...,\mathbf{b}_m$, $\mathbf{b}_k = (b_{k1}...b_{kn})$ spans an m-dimensional subspace P of the n-dimensional space B of all n-channel signals, which we will call a signal space. An n-channel signal means the set of outputs of n magnetic field sensors, either from an actual measurement or due

to a given source.

There exists a projection operator **P** such that $\mathbf{Pb} \in P$ for any $\mathbf{b} \in B$. If we have determined an orthonormal basis $\mathbf{u}_1 ... \mathbf{u}_m$, $\mathbf{u}_j^T \mathbf{u}_k = \delta_{jk}$, for P we find $\mathbf{P} = \mathbf{U}\mathbf{U}^T$, $\mathbf{U} = (\mathbf{u}_1 ... \mathbf{u}_m)$, i.e., **U** is the matrix whose columns are the basis vectors. The required orthonormal basis can be found, e.g., with Gram-Schmidt orthogonalization. However, to obtain a measure of the linear independence of $\mathbf{b}_1,...,\mathbf{b}_m$, it is most convenient to use the singular-value decomposition of $\mathbf{B} = (\mathbf{b}_1 ... \mathbf{b}_m) = \mathbf{U}\Lambda\mathbf{V}^T$. The orthonormal basis is given in **U** while small singular values in Λ indicate linear dependence.

Once **P** has been found we can multiply our measured data $\mathbf{b}(t)$ by either **P** or **I** - **P** thereby restricting the analysis to P or its orthogonal complement subspace, respectively. We denote the projection by $\mathbf{b}_{||} = \mathbf{Pb}$ and the orthogonal complement projection by $\mathbf{b}_\perp = (\mathbf{I} - \mathbf{P})\mathbf{b}$. Clearly, the projection $\mathbf{b}_{||}$ is the part of **b** expressible as a linear combination of $\mathbf{b}_1,...,\mathbf{b}_m$ while $\mathbf{b}_\perp = \mathbf{b} - \mathbf{b}_{||}$ is the remainder after an optimal subtraction of the component lying in P. Once a projection is defined it is important to apply it to the model data about to be compared with $\mathbf{b}_\perp$ as well.

In time-varying fixed dipole modelling, P is spanned by the signals produced by dipoles at known locations and orientations. The result of the analysis is expressed as time varying optimal weights $\mathbf{q}(t) = (\mathbf{q}_1(t),...,\mathbf{q}_m(t))$ of $\mathbf{b}_1,...,\mathbf{b}_m$, obtained by multiplying $\mathbf{b}(t)$ by the pseudoinverse of **B**, $\mathbf{B}^+ = \mathbf{V}\Lambda^{-1}\mathbf{U}^T$. Now, multiplying $\mathbf{q}(t) = \mathbf{B}^+\mathbf{b}(t)$ by **B** we arrive at $\mathbf{b}_{||}(t) = \mathbf{U}\mathbf{U}^T\mathbf{b}(t) = \mathbf{Pb}(t)$. We may consider $\mathbf{Pb}(t)$ as a spatial filter whose output can be expressed either in the signal space as $\mathbf{b}_{||}(t)$ or in terms of $\mathbf{q}(t)$ in the source space. However, the term source space may be misleading since we can compute $\mathbf{q}(t)$ for any set $\mathbf{b}_1,...,\mathbf{b}_m$, even though we are not able to find the actual source configuration corresponding to all or some of $\mathbf{b}_1,...,\mathbf{b}_m$. With known dipoles as sources we might also use different conductor models depending on the source location. For example, the simple sphere model is an accurate description for the superficial sources while we may have to resort to a realistically shaped model to correctly account for deep sources.

Applications

Both $\mathbf{b}_{||}$ and $\mathbf{b}_\perp$ can be useful in the analysis. For example, we can do noise cancellation beyond that provided by our first-order gradiometers, which are not sensitive to a homogeneous field but detect homogeneous gradients and higher-order derivatives. The first spatial derivatives of the magnetic field **B** can be conveniently expressed as a 3 x 3 matrix:

$$\mathbf{G} = \begin{pmatrix} \frac{\partial B_x}{\partial x} & \frac{\partial B_x}{\partial y} & \frac{\partial B_x}{\partial z} \\ \frac{\partial B_y}{\partial x} & \frac{\partial B_y}{\partial y} & \frac{\partial B_y}{\partial z} \\ \frac{\partial B_z}{\partial x} & \frac{\partial B_z}{\partial y} & \frac{\partial B_z}{\partial z} \end{pmatrix}$$

However, we always have $\nabla \cdot \mathbf{B} = 0$. Since we are dealing with a slowly varying field, the quasi-static approximation applies and, consequently, $\nabla \times \mathbf{B} = 0$ in the current-free region outside the head. These two Maxwell's equations imply that only five of the components of **G** are independent. If now $\mathbf{b}_1,...,\mathbf{b}_m$ are the m=5 independent homogeneous gradient components as seen by our sensors, $\mathbf{b}_\perp$ denotes data from which the contribution of homogeneous gradients, i.e., fields from distant noise sources is removed.

Sometimes we can also gain more insight to the multiple-source identification problem by projecting out the fields of a set of dipoles first. If an eye-blink artefact is inevitable, it is possible to remove its contribution and reveal the underlying field from cerebral sources.

As an example, consider the case of fitting the two auditory N100m sources discussed above. We can start our analysis by fitting a single source to explain one half of the data first. We have noticed that a selection of a channel subset is not really necessary at this point; the source location given by this 'blind' single ECD fitting is going to be approximately correct. After finding the first source, we construct the corresponding orthogonal complement projection and fit a new dipole to the remaining $\mathbf{b}_\perp$. As a result of this procedure we have two good initial guesses available for the final two-dipole fitting routine.

The projection to a given subspace $\mathbf{b}_{||}$ can also be applied to the analysis of single trials. It might be, for example, possible to classify single trials according to the amplitude of $\mathbf{b}_{||}(t)$.

Examples of results

Somatosensory evoked fields

Earlier MEG studies of somatosensory evoked responses have revealed three clearly separate source areas: the first somatosensory cortex SI, activated contralaterally with respect to the stimulated part of the body, and the two second somatosensory cortices, SII, activated nearly symmetrically, independent of the side of the stimulus.

When we carried out experiments with our whole cortex system using median nerve stimulation, it was readily evident that an additional source area, posterior to SI was present (figure 4). A more careful analysis showed that the time dependence of the activity at this area is clearly different from the areas identified earlier

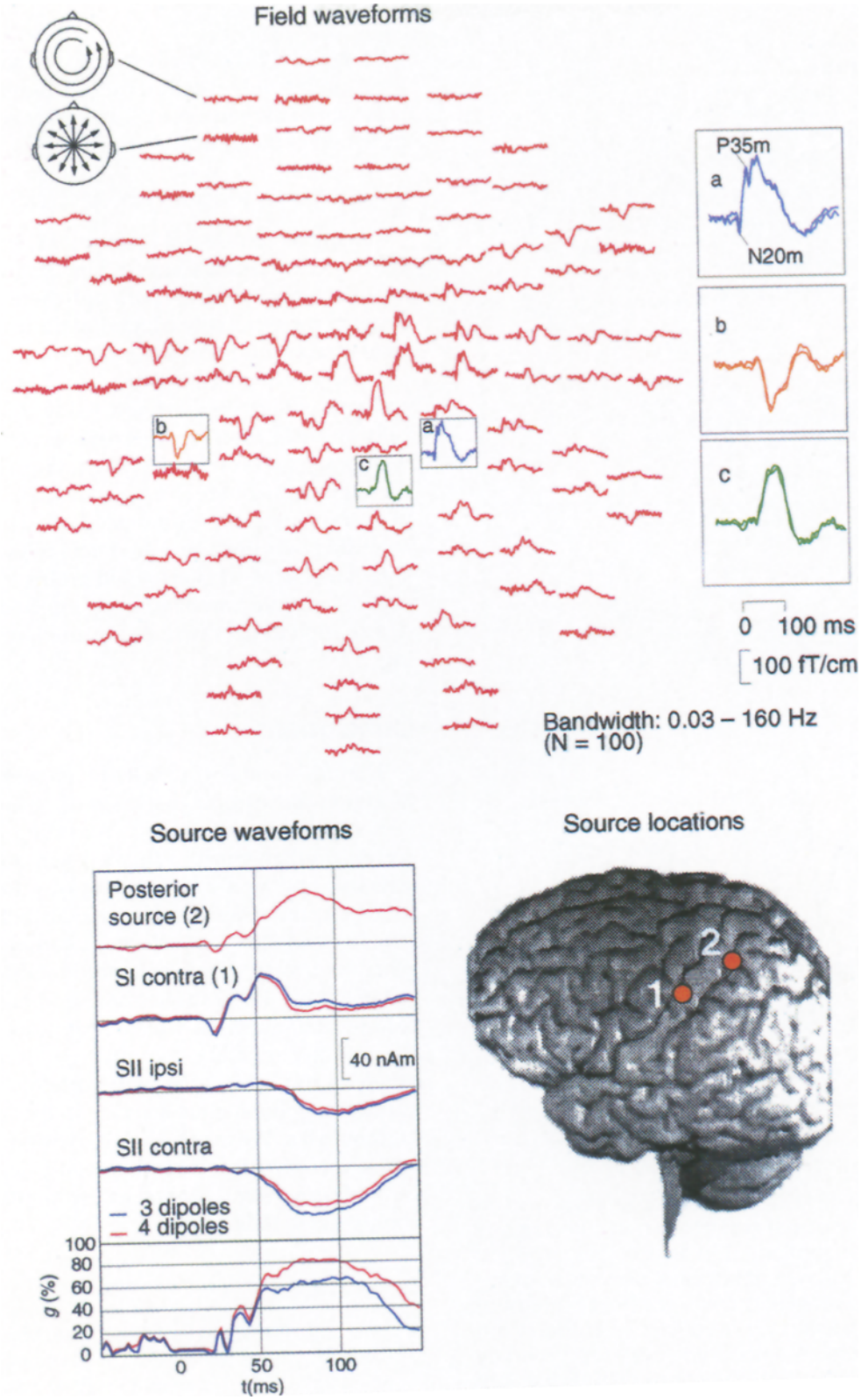

Figure 4. Somatosensory evoked responses to left median nerve stimulation. Above: The measured field waveforms with representative SI (a), SII (b), and posterior parietal (c) waveforms shown in the inset. Below left: Results of time-varying dipole modelling. Data with all four active sources are shown in red whereas the blue waveforms indicate results from a three-dipole model with the posterior source omitted. Below right: The SI (1) and posterior (2) source locations superimposed on a three-dimensional MRI surface reconstruction.

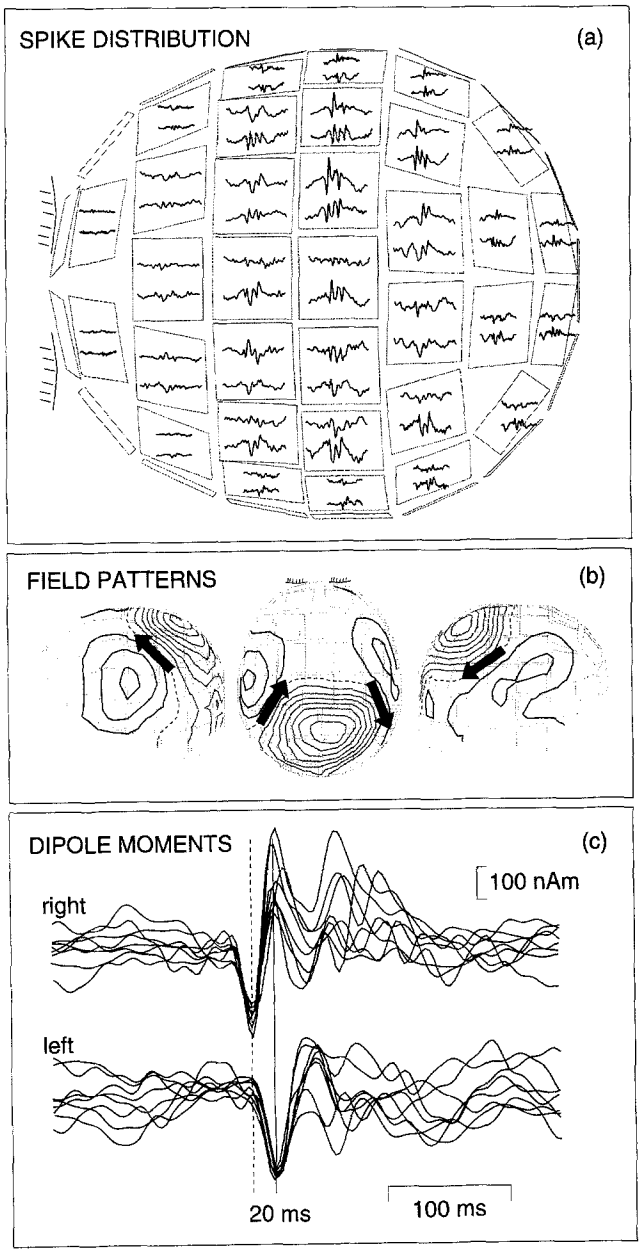

Figure 5. (a) Spatial distribution of one spike displayed on the sensor array; only about half of the measured signals are shown in this projection. The two traces on each sensor unit illustrate the two orthogonal derivatives of the magnetic field that were measured. (b) Field patterns at the time instant indicated by a vertical solid line in the lower part of the figure. The isocontours are separated by 400 fT. (c) Dipole moments as a function of time in the right and left hemispheres. Each trace corresponds to one unaveraged spike, whose field distribution was explained by a two-dipole model.

(Forss et al. 1994). Furthermore, the source in this new area is independent of the others in the sense that the time behavior of the sources at SI and SII is not affected by the inclusion of the fourth source.

Symmetrically located epileptic activity

Owing to comissural connections, interictal epileptic activity is sometimes seen in homologous cortical areas in both hemispheres, even though there might be a single primary focus initially triggering the activity. In presurgical evaluation it is thus indispensable to identify the primarily active hemisphere. In a recent study of an epileptic patient we were able to identify two symmetrically located sources in the parietal cortex with different temporal patters of activity, indicating a primary focus in the right hemisphere (Hari et al. 1994). The data shown in figure 5 clearly demonstrate that a whole-cortex recording was necessary to detect reliably both sources simultaneously. It is also evident that the approximate source locations can be directly inferred from the spike distribution in the raw data, without any signal averaging.

Conclusions

The development of SQUID magnetometers for the detection of neuromagnetic signals has reached an important and essential goal: recording over the whole cortex simultaneously. While present systems are highly sensitive and produce a wealth of reliable data, more refined approaches are required in both forward and inverse modelling as well as in combining MEG with other noninvasive methods, most notably EEG and MRI.

Up to now, MEG studies have emphasized the ability to locate the sources of evoked responses. However, with the unique possibility to record signals quickly over the whole cortex, the focus will certainly move towards studies of spontaneous activity and its changes during various tasks. We expect that the neuromagnetic method will show its usefulness especially in basic research through carefully designed experiments analyzed with sophisticated tools.

References

Ahonen, A.I., Hämäläinen, M.S., Kajola, M.J., Knuutila, J.E.T., Laine, P.P., Lounasmaa, O.V., Parkkonen, L.T., Simola, J.T. and Tesche, C.D. 122-channel SQUID instrument for investigating the magnetic signals from the human brain. Physica Scripta, 1993a, T49: 198-205.

Ahonen, A.I., Hämäläinen, M.S., Ilmoniemi, R.J., Kajola, M.J., Knuutila, J.E.T., Simola, J.T. and Vilkman, V.A. Sampling theory for neuromagnetic detector arrays. IEEE. Trans. Biomed. Eng., 1993b, 40: 859-869.

Forss, N., Hari, R., Salmelin, R., Ahonen, A., Hämäläinen, M., Kajola, M., Knuutila, J. and Simola, J. Activation of the human posterior parietal cortex by median nerve stimulation. Exp. Brain Res., 1994, 99: 309-315.

Golub, G.H. and van Loan, C.F. Matrix computations, 2nd Ed. The Johns Hopkins University, Baltimore, 1989.

Hämäläinen, M.S. and Sarvas, J. Realistic conductivity geometry model of the human head for interpretation of neuromagnetic data. IEEE Trans. Biomed. Eng., 1989, 36: 165-171.

Hari, R., Ahonen, A., Forss, N., Granström, M.-L., Hämäläinen, M., Kajola, M., Knuutila, J., Lounasmaa, O.V., Mäkelä, J.P., Paetau, R., Salmelin, R. and Simola, J. Parietal epileptic mirror focus detected with a whole-head neuromagnetometer. NeuroReport, 1993, 5: 45-48.

Mosher, J.C., Lewis, P.S. and Leahy, R. Multiple dipole modeling and localization from spatio-temporal MEG data. IEEE Trans. Biomed. Eng., 1992, 39: 541-557.

Salmelin, R., Hari, R., Lounasmaa, O.V. and Sams M. Dynamics of brain activation during picture naming. Nature, 1994, 368: 463-465.

Scherg, M. Fundamentals of dipole source potential analysis. In: F. Grandori, M. Hoke and G.L. Romani (Eds.), Auditory Evoked Magnetic Fields and Electric Potentials. Adv. Audiol., Vol. 6., Basel, Karger, 1990: 40-69.

Seppä, H., Ahonen, A., Knuutila, J., Simola, J. and Vilkman, V. Dc-SQUID electronics based on adaptive positive feedback: Experiments. IEEE Trans. Magn., 1991, 27: 2488-2490.

Uusitalo, M.A., Ilmoniemi, R.J. and Tesche, C.D. The signal-space projection (SSP) method. International Society for Brain Electromagnetic Topography. 5th International congress, 1995, Vol 7(4): 340.